

Determination of the b -quark mass m_b from the angular screening effects in the ATLAS b -jet shape data.

Javier Llorente, Josu Cantero

*Universidad Autónoma de Madrid (UAM), Facultad de Ciencias.
Departamento de Física Teórica. Cantoblanco, Madrid 28049, Spain*

Abstract

The dependence of jet shapes in $t\bar{t}$ events on the b -quark mass and the strong coupling is investigated. To this end, the PYTHIA Monte Carlo generator is used to produce samples of $t\bar{t}$ events in pp collisions at $\sqrt{s} = 7$ TeV, performing a scan over the values for the shower QCD scale Λ_s and the b -quark mass m_b . The obtained jet shapes are compared with recently published data from the ATLAS Collaboration. From fits to the light-jet data, the Monte Carlo shower scale is determined, while the b -quark mass is extracted using the b -jet shapes. The result for the mass of the b -quark is $m_b = 4.86^{+0.49}_{-0.42}$ GeV.

1. Introduction

It is a well established fact that hadrons produced in e^+e^- , ep and pp colliders at high momentum transfers appear in well collimated bundles called jets. These jets are understood to proceed via a two step process. The first one, which is of a perturbative nature, relates to the formation of a parton shower following the underlying hard partonic interaction. The second, which is non-perturbative, is called hadronisation and relates to the way partons in the shower recombine to form colourless hadrons. Hadronisation effects are expected to become smaller at higher transverse momentum scales.

Jet shapes [1, 2] are defined as the normalised transverse momentum flow as a function of the distance to the jet axis. They are considered to be a measure of the jet internal structure. Thus, at high energies, they are sensitive to the amount of final state radiation.

Recently, the ATLAS Collaboration has published data on b -jet and light jet shapes measured in $t\bar{t}$ final states [3]. Here b -jets arise from the decays $t \rightarrow Wb$ in both the single-lepton and dilepton

☆

Email addresses: javier.llorente.merino@cern.ch (Javier Llorente), josu.cantero.garcia@cern.ch (Josu Cantero)

Preprint submitted to Nuclear Physics B

November 6, 2014

modes. Light jets are studied in the single lepton channel, where one W is decaying leptonically and the second one hadronically. It is found that b -jets are broader than light jets.

This is understood to be due to the fact that the angular radiation pattern for a b -quark is significantly different than that of a light-quark due to the heavier mass of the former. These effects were thoroughly studied in Ref. [4] for the full angular range subtended from the direction of motion of the b -quark.

Indeed, for a parton branching $q \rightarrow \bar{q}g$, the invariant mass of the decay products can be written as $m_q^2 \simeq 2E_{\bar{q}}E_g(1 - \cos \theta)$ in the regime where the quark mass is negligible compared to its energy scale. Here θ is the angle formed by the 3-momenta of the final-state quark and the radiated gluon. In the collinear limit, valid for the jet cone region, one can expand the cosine as a Taylor series and easily obtain the relation

$$\theta \simeq \frac{m_q}{\sqrt{E_{\bar{q}}E_g}} = \frac{1}{\sqrt{z(1-z)}} \frac{m_q}{E_q} \quad (1)$$

Here, z is the fraction of energy carried by the gluon ($E_g = zE_q$). Eq. 1 suggests that there is a direct relationship between the mass of the branching parton and the angular distribution of the resulting products around the jet axis. For light-quark jets, the dominant effect on the opening angle described by Eq. 1 arises from the gluon energy fraction $0 < z < 1$. On the other hand, the opening angle in b -jets is controlled by the heavier mass of the b -quark.

Defining $\theta_0 = m_q/E_q$, the probability of a gluon emission at a small opening angle $\theta < \theta_0 \ll 1$ is given by [5]

$$\left(\frac{d\sigma}{d\omega}\right)_{q \rightarrow \bar{q}g} = \frac{\alpha_s C_F}{\pi\omega} \frac{(2 \sin \theta/2)^2 d(2 \sin \theta/2)^2}{[(2 \sin \theta/2)^2 + \theta_0^2]^2} [1 + O(\theta_0, \omega)] \sim \frac{1}{\omega} \frac{\theta^2 d\theta^2}{[\theta^2 + \theta_0^2]^2} \quad (2)$$

In Eq. 2, ω corresponds to the energy of the radiated gluon. From here one can infer that for the kinematical region with $\theta < \theta_0$ the amount of radiation is highly suppressed. This effect is known as angular screening, and the region $\theta < \theta_0$ is known as the ‘dead cone’.

This discussion proves interesting to investigate the dependence of the b -jet shapes on the b -quark mass. This is the purpose of this paper. To this end, the PYTHIA Monte Carlo program [6] was used to generate samples of $t\bar{t}$ events where both the shower scale Λ_s and the b -quark mass m_b were varied in the ranges [20, 300] MeV and [4, 6] GeV respectively. In this study, only the first three p_T bins studied in [3] are introduced into the fits. This is done to maximise the effect of the b -quark mass in the jet shapes, which is largely reduced at high p_T because of the inverse proportionality of θ_0 with the energy of the parent quark. The outline of the paper is as follows: the MC predictions are discussed in Sect. 2. In Sect. 3 the jet selection and the jet shape definition are discussed. The fitting procedure is addressed in Sect. 4, while Sections 5 and 6 are dedicated to the extraction of Λ_s and m_b , respectively. In Section 7, the theoretical uncertainties are described. Finally, Section 8 is left for summary and conclusions.

2. Monte Carlo predictions

Top-quark pair events have been generated using the PYTHIA 6.4 program. Additionally, the MSTJ(42)=3 switch has been used to take into account the larger mass of the b -quark on the angular distribution of the decay products [7]. Also, the switch MSTJ(43)=3 has been used to set the fragmentation variable z as the fraction of energy in the centre-of-mass frame of the showering partons [6].

Jet shapes naturally depend on the strong coupling constant α_s , as it controls the radiation emitted by strongly-interacting partons, and have been in fact a precise way to determine its value in Ref. [8]. Therefore, one needs to take this effect into account for a precise determination of the b -quark mass. At the one-loop order, the scale dependence of the strong coupling can be parametrised by [13]

$$\alpha_s(Q^2) = \frac{1}{\beta_0 \log\left(\frac{Q^2}{\Lambda^2}\right)}; \quad \beta_0 = \frac{1}{4\pi} \left(11 - \frac{2}{3}n_f\right) \quad (3)$$

Eq. 3 incorporates the QCD scale Λ , which can be varied for the PYTHIA time-like parton showers arising from a resonant decay using the PARJ(81) switch. Finally, the b -quark mass m_b is varied around its nominal value $m_b = 4.8$ GeV using the PMAS(5) and PARF(105) switches, which control the kinematical mass of the b -quark and its constituent mass, respectively. Additionally, $t\bar{t}$ samples have been generated using the HERWIG++ Monte Carlo program [9]. The differences between the value of m_b obtained in HERWIG++ and that obtained using PYTHIA will be discussed later, and assigned as a theoretical uncertainty.

3. Jet selection and jet shape calculation

The final-state particles from the PYTHIA simulation are clustered using the anti- k_t algorithm [14] as implemented in FASTJET [15], with a radius parameter $R = 0.4$. As specified in Ref. [3], muons and neutrinos are left out of the clustering algorithm.

All jets with transverse momentum $p_T > 30$ GeV are pre-selected. To select the jets induced by b -quarks from the top decays, a matching procedure is used between the clustered jets and any hadron containing b -quarks. If one of these hadrons with $p_T > 5$ GeV is found at a distance $\Delta R = \sqrt{(\Delta\eta)^2 + (\Delta\phi)^2} < 0.3$ from the axis of a given jet, this jet is selected as a b -jet. Alternatively, light-quark jets are selected as the pair of jets which, not containing B -hadrons closer than $\Delta R = 0.3$ to the jet axis, have the closest invariant mass to the nominal W boson mass $m_W = 80.4$ GeV.

The differential jet shape is then calculated for both samples following the formula in [3]

$$\langle \rho(r) \rangle = \frac{1}{\Delta r} \frac{1}{N_{\text{jets}}} \sum_{\text{jets}} \frac{p_T(r - \Delta r/2, r + \Delta r/2)}{p_T(0, R)} \quad (4)$$

4. Analysis procedure

As b -jet shapes depend on both the parton shower QCD scale Λ_s and the b -quark mass m_b , both need to be determined for a precise result. A simultaneous determination of both parameters is not possible because a variation of one of them can be compensated by an opposite variation of the other one, leading to a set of degenerate minima in the plane (m_b, Λ_s) . However, it is expected that the light-jet shapes in [3] depend only in Λ_s and not in m_b . Therefore, one can determine the parameter Λ_s from the light-jet shapes and use it for the extraction of m_b from the b -jet data.

The method used for the extraction of a physical parameter $\beta = \Lambda_s, m_b$ from a theoretical distribution scan relies on the minimisation of a standard χ^2 for each p_T bin using MINUIT [16]. The χ^2 function is defined in a way which takes into account the correlations between the experimental uncertainties via a set of nuisance parameters $\{\lambda_i\}$. In terms of the parameter β to be extracted and the nuisance parameter vector $\vec{\lambda}$, it can be written as

$$\chi^2(\beta; \vec{\lambda}) = \sum_k \frac{(x_k - F_k(\beta; \vec{\lambda}))^2}{\Delta x_k^2 + \Delta \tau_k^2} + \sum_i \lambda_i^2 \quad (5)$$

$$F_k(\beta; \vec{\lambda}) = \phi_k(\beta) \left(1 + \sum_i \lambda_i \sigma_{ik} \right) \quad (6)$$

In Eq. 5, the index k runs over all r bins in a given p_T bin, with a given value x_k of the jet shape and with statistical uncertainty Δx_k . Here, $\Delta \tau_k$ represents the statistical uncertainty on the theoretical predictions. The nuisance parameters λ_i , one for each source of uncertainty, are also involved in Eq. 6, where the functions $\phi_k(\beta)$ correspond to the nominal dependence of the jet shape with the parameter β in bin k . They are parametrised in terms of a parabola throughout this paper. Finally, σ_{ik} are the relative uncertainties for source i in the bin k [12].

Each nuisance parameter corresponds to a different uncertainty on the data. Table 1 shows the identification of each λ_i with the corresponding source, ordered from larger to smaller impact.

Table 1: Identification of the nuisance parameters λ_i with the sources of experimental uncertainty in the ATLAS data.

Nuisance parameter	Source of uncertainty	Impact on data
λ_1	Pileup	2% – 10%
λ_2	Cluster systematics	2% – 10%
λ_3	Unfolding-modelling	1% – 8%
λ_4	Jet energy scale	$\simeq 5\%$
λ_5	Jet energy resolution	$\simeq 5\%$
λ_6	JVF	< 1%

5. Determination of the parton shower scale Λ_s

In order to determine the QCD scale of the parton shower Monte Carlo which best fits the jet shape data, the dependence of the light-quark jet shapes on Λ_s is studied. Figure 1 shows the comparison of the light-jet shape data in [3] and the PYTHIA expectations for several values of Λ_s . The dependence of the jet shapes on Λ_s is clearly seen from the figure.

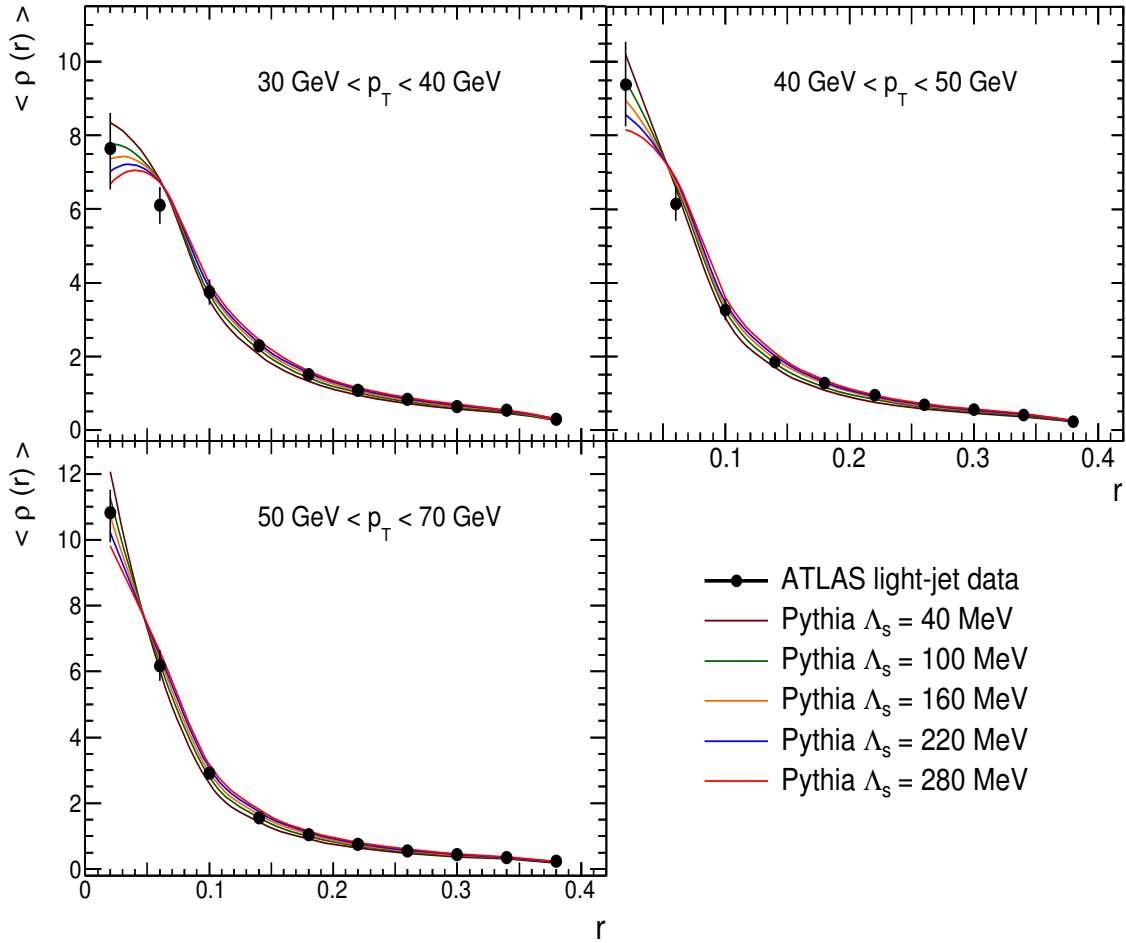


Figure 1: Results of the Λ_s scan compared to the ATLAS light-jet data in [3]

In order to parametrise this dependence and obtain the interpolating functions $\phi_k(\Lambda_s)$ in Eq. 6, samples with Λ_s varying from 20 MeV to 300 MeV in steps of 20 MeV have been generated. To illustrate this dependence, Figure 2 shows the points obtained from this scan together with the fitted functions $\phi_k(\Lambda_s)$ for $r = 0.02$ in each p_T bin.

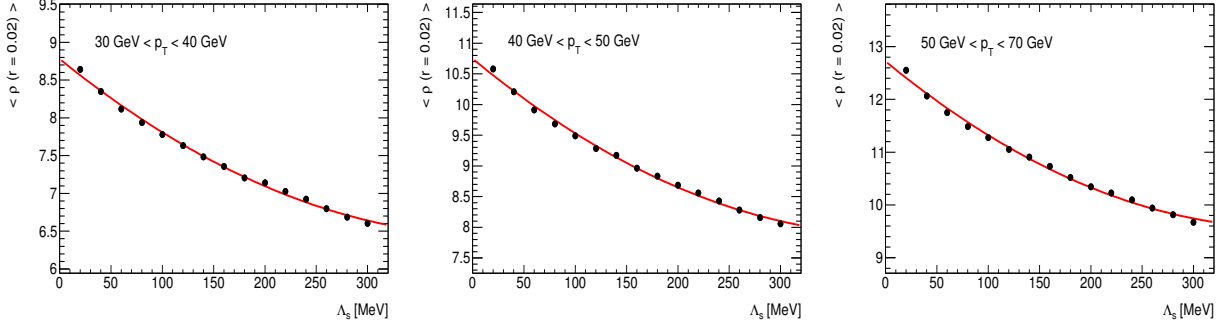


Figure 2: Dependence of the light-quark jet shape $\langle \rho(r = 0.02) \rangle$ with the parton shower scale Λ_s for the p_T intervals $30 \text{ GeV} < p_T < 40 \text{ GeV}$ (left), $40 \text{ GeV} < p_T < 50 \text{ GeV}$ (middle) and $50 \text{ GeV} < p_T < 70 \text{ GeV}$ (right), together with the interpolating functions $\phi_k(\Lambda_s)$.

The fits using Eqs. 5 and 6 have been performed for every p_T bin separately, and finally all of them are combined into a global fit to the three bins with $30 \text{ GeV} < p_T < 70 \text{ GeV}$. Fig. 3 shows the values of the nuisance parameters $\{\lambda_i\}$ involved in the fit, as well as the correlation matrix between them. The values of the nuisance parameters are always compatible with the $\pm 1\sigma$ band, fact which gives us confidence on the quality of the fit. The results of the fits to Λ_s are summarised in Table 2, together with the fit uncertainties and the values of χ^2/N_{dof} .

Table 2: Summary of the results of the fit for Λ_s using the light-jet shape data.

Bin	Λ_s value (MeV)	Fit error (MeV)	χ^2/N_{dof}
$30 \text{ GeV} < p_T < 40 \text{ GeV}$	187.5	24.0	10.6 / 9
$40 \text{ GeV} < p_T < 50 \text{ GeV}$	193.5	24.2	11.0 / 9
$50 \text{ GeV} < p_T < 70 \text{ GeV}$	137.7	17.3	7.8 / 9
Global fit	162.1	9.6	39.0 / 29

The nominal results obtained here have been derived using the one-loop solution to the renormalisation group equation (RGE) for the PYTHIA parton shower. In addition, the values of Λ_s have also been extracted using HERWIG++ with the solutions to the RGE implemented up to two loops. The resulting value at one loop is $\Lambda_s = 160.7 \pm 15.3 \text{ MeV}$, in good agreement with the nominal value quoted above. For the two-loop case, the expression for the running strong coupling is [13]

$$\alpha_s(Q^2) = \frac{1}{\beta_0 \log x} \left[1 - \frac{\beta_1}{\beta_0^2} \frac{\log(\log x)}{\log x} \right]; \quad x = \frac{Q^2}{\Lambda^2} \quad (7)$$

where β_0 is given in Eq. 3 and $\beta_1 = \frac{1}{(4\pi)^2} (102 - \frac{38}{3}n_f)$. In this case, a value of $\Lambda_s = 276.1 \pm 17.3 \text{ MeV}$ is obtained, which is compatible with the value quoted in Ref. [17] within the uncertainties. The effect of the two-loop running of the shower α_s on the b -quark mass will be explained in Sect. 7.5.

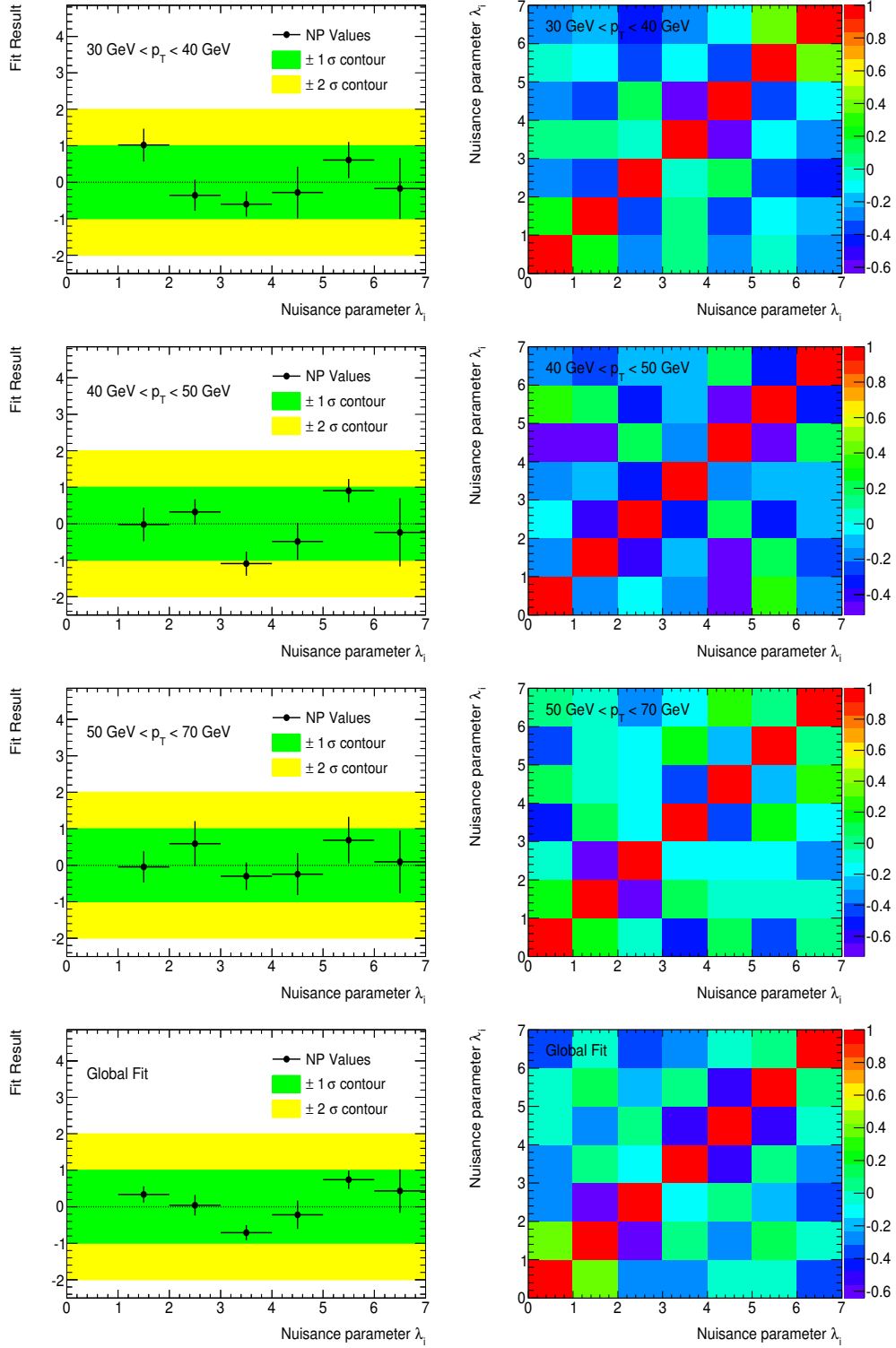


Figure 3: Results for the nuisance parameters involved in the Λ_s extraction (left column) and correlation matrices between them (right column) for each p_T bin considered. The results obtained for the global fit are shown at the bottom row.

6. Determination of the b -quark mass m_b

Once the parton shower scale Λ_s is determined, the result is used to generate PYTHIA samples with several different values of the b -quark mass. The scan is performed in this case by varying this parameter from 4.0 GeV to 6.0 GeV in steps of 250 MeV. Figure 4 shows the comparison of the ATLAS b -jet shape data with the expectations from PYTHIA for several values of m_b , including those for $m_b = 3.0$ and 7.0 GeV. The value of the parton shower scale for the predictions shown in Fig. 4 is the one corresponding to the global fit to the light-jet shape data, namely $\Lambda_s = 162.1 \pm 9.6$ MeV. The dependence of the jet shapes with the b -quark mass is more marked than in the case of Λ_s , providing high precision to the m_b determination.

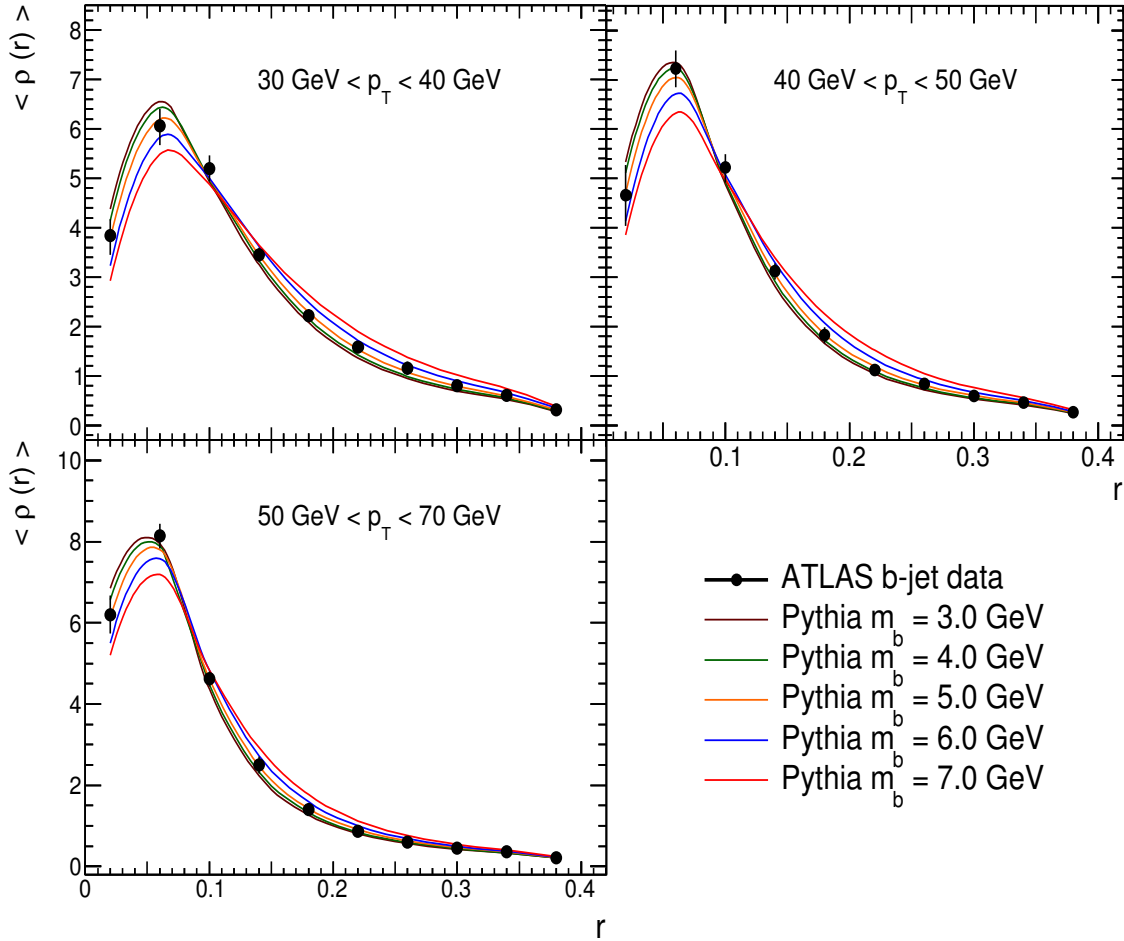


Figure 4: Results of the m_b scan compared to the ATLAS b -jet data in [3]. The QCD scale involved in the parton shower has been taken to be the one corresponding to the global fit to the light-jet data, $\Lambda_s = 162.1 \pm 9.6$ MeV

The b -jet shapes show a turn-over close to the jet cores due to the angular screening caused by the heavy mass of the b -quark. The larger m_b is, the wider is the jet in the sense that the inner

core has smaller energy deposits. The description of all bins provided by PYTHIA is excellent, showing that it is possible to perform a safe fit to the data. The parametrisation of the interpolating functions $\phi_k(m_b)$ describing the dependence of the differential b -jet shapes with the b -quark mass is done using second-order polynomials as in the case of the shower scale Λ_s . Figure 5 shows the dependence for $r = 0.02$ in each p_T bin, as predicted by PYTHIA

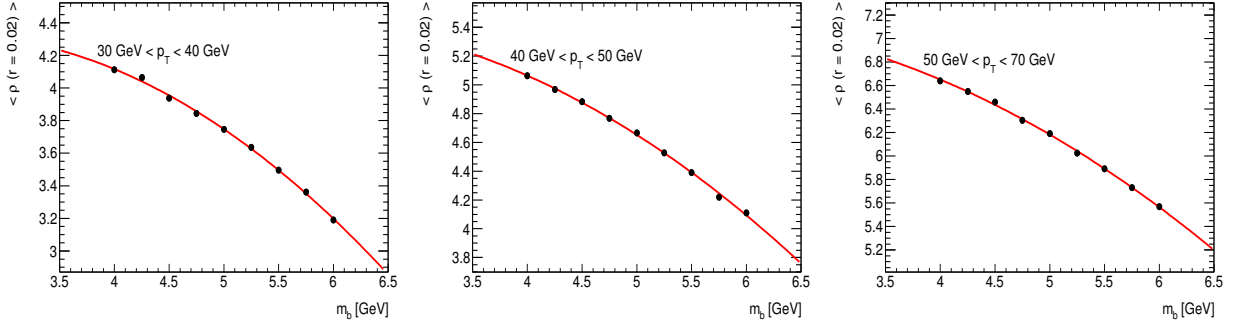


Figure 5: Dependence of the b -quark jet shape $\langle \rho(r = 0.02) \rangle$ with the b -quark mass m_b for the p_T intervals $30 \text{ GeV} < p_T < 40 \text{ GeV}$ (left), $40 \text{ GeV} < p_T < 50 \text{ GeV}$ (middle) and $50 \text{ GeV} < p_T < 70 \text{ GeV}$ (right), together with the interpolating functions $\phi_k(m_b)$.

The global fit has been performed including all p_T bins and using the global value of the parton shower scale, $\Lambda_s = 162.1 \pm 9.6 \text{ MeV}$. As a cross-check, for each p_T bin, extra samples have been generated using the partial values of Λ_s shown in Table 2. The agreement between all the extracted values of m_b is excellent, as can be seen in Table 3.

Table 3: Summary of the results of the fits for m_b using the b -jet shape data and the corresponding value of Λ_s for each bin listed in table 2. The global fit is performed using the globally extracted value of the parton shower scale $\Lambda_s = 162.1 \text{ MeV}$.

Bin	m_b value (GeV)	Fit error (GeV)	χ^2/N_{dof}
$30 \text{ GeV} < p_T < 40 \text{ GeV}$	5.00	0.14	8.28 / 9
$40 \text{ GeV} < p_T < 50 \text{ GeV}$	4.82	0.19	10.41 / 9
$50 \text{ GeV} < p_T < 70 \text{ GeV}$	4.82	0.13	11.99 / 9
Global fit	4.86	0.08	43.04 / 29

As before, the values of the nuisance parameters and the correlation matrices between them are shown in Figure 6 for the fits performed using each extracted value of the shower scale. As in the previous case, we find that the nuisance parameters are well behaved, being always compatible with the $\pm 1\sigma$ contour band. This is specially important for the global fit, as its result will be taken as the central value for our determination. As can be seen in the lower part of Figure 6, the behaviour of the fit parameters is very good.

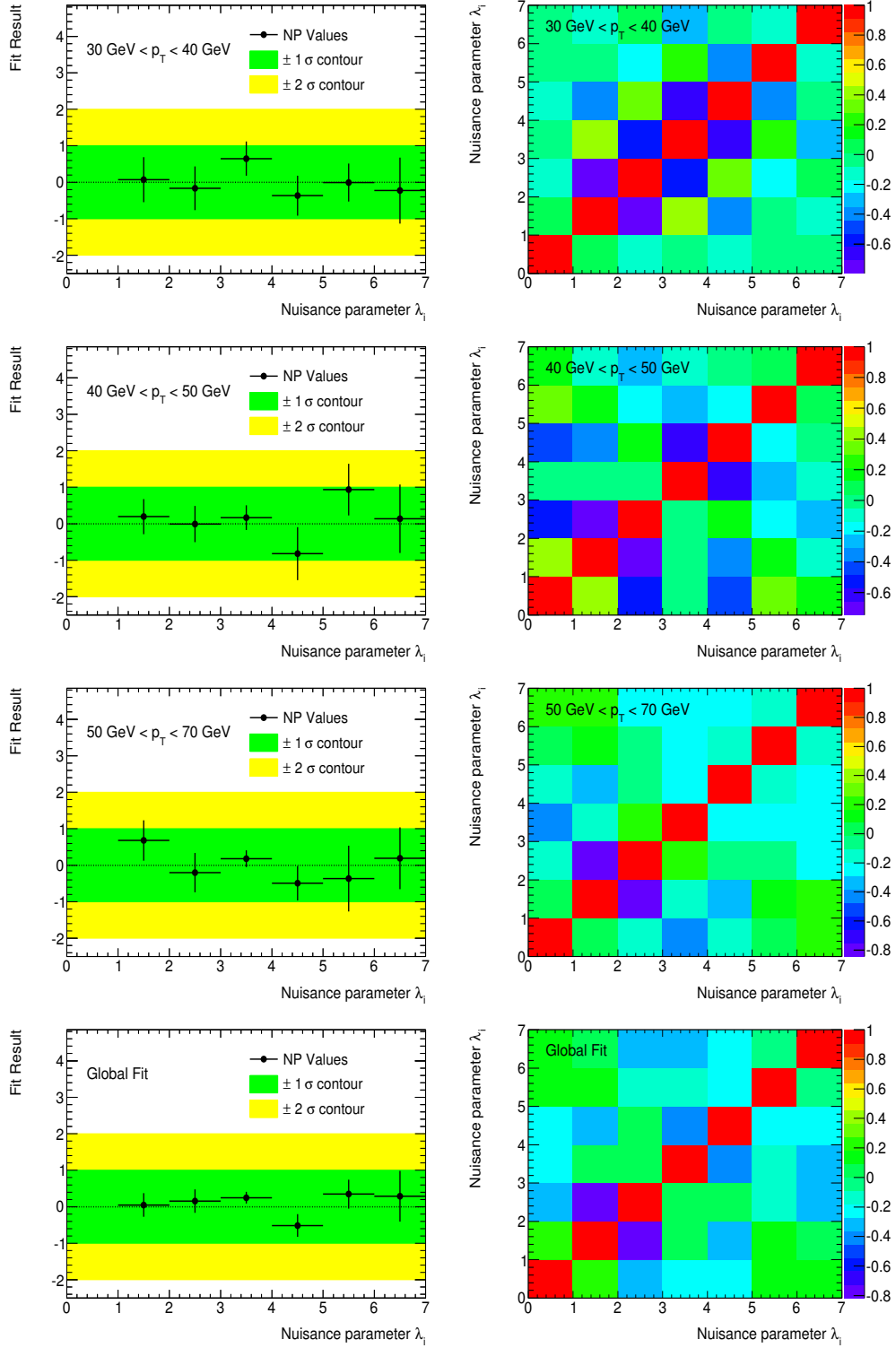


Figure 6: Results for the nuisance parameters involved in the m_b extraction (left column) and correlation matrices between them (right column) for each p_T bin considered. The results obtained for the global fit are shown at the bottom row. For each p_T bin, the corresponding value of Λ_s listed in Table 2 has been used. For the global fit, the globally extracted value is $\Lambda_s = 162.1$ MeV.

7. Theoretical uncertainties

In this section, the uncertainties on the theory are discussed. They come from several sources, including the modelling of the parton shower, hadronisation and multiple parton interactions. Other effects such as the amount of initial and final-state radiation, the colour reconnection model and the error on the determination of the parton shower scale Λ_s are also studied. The generator modelling uncertainty is the main source of uncertainty for these analysis, not being greater than 400 MeV in terms of the extracted b -quark mass. All variations of the theoretical distributions are performed with respect to the nominal sample, produced using the fitted values of Λ_s and m_b .

7.1. Generator modelling

The PYTHIA predictions use virtuality-ordered parton showers and the Lund string model for the hadronisation. In order to study the impact of this choice on the extraction of m_b , a sample of $t\bar{t}$ events has been generated using the HERWIG++ Monte Carlo program [9], which incorporates angular-ordered parton showers as well as the cluster hadronisation model. The modelling of the underlying event (multiparton interactions) is also different between both approaches. For HERWIG++, the LHC-UE7-2 tune has been chosen. This is based on the ATLAS measurements of the underlying event using charged particles [18]. On the other hand, PYTHIA uses the so-called TUNE A as default [19], which is based on the correct description of many Tevatron measurements.

In Figure 7, the nominal prediction by PYTHIA is compared to the nominal predictions by HERWIG++.

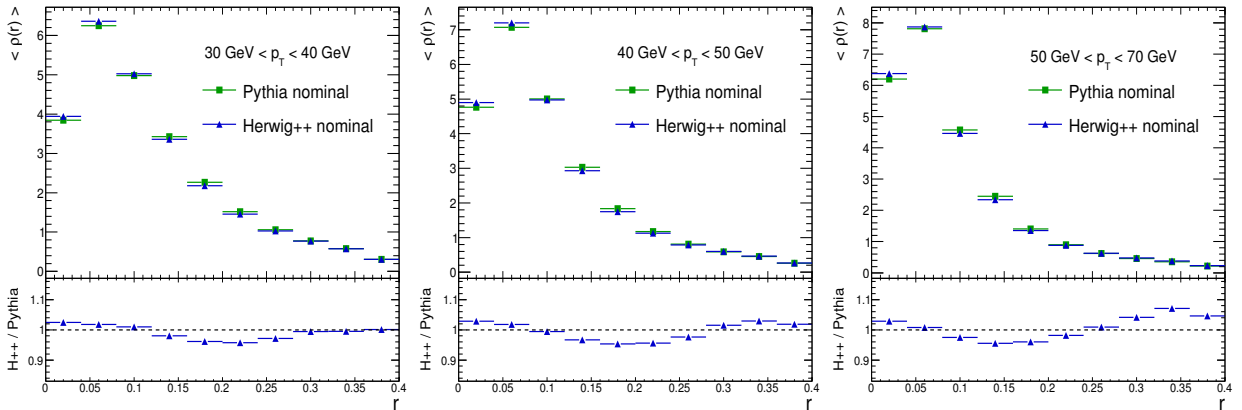


Figure 7: The difference between the PYTHIA and HERWIG++ predictions for the fitted values $m_b = 4.86$ GeV and $\Lambda_s = 162.1$ MeV. This difference, arising from the parton shower and hadronisation, is the source of the theoretical uncertainty due to the generator modelling.

In order to study the impact of these differences on the determination of m_b , the full analysis has been repeated using HERWIG++. In this case, the b -quark mass is scanned by varying both the NOMINALMASS and the CONSTITUENTMASS flags for /HERWIG/PARTICLES/B and /HERWIG/PARTICLES/BBAR. The value of Λ_s has been set to 160.7 ± 15.3 MeV, which is the value obtained in Section 5 for the HERWIG++ approach. The result for the b -quark mass is $m_b = 5.25 \pm 0.09$ GeV, and the difference with respect to the nominal value is symmetrised and ascribed as a theoretical uncertainty.

7.2. Initial-state radiation

The amount of initial-state radiation (ISR) can lead to differences in the jet shapes. To test this effect, two additional samples with reduced and enhanced levels of ISR are generated. The ISR is controlled in PYTHIA using the parameters PARP(67) and PARP(64). To decrease the ISR, the parameters are set to 0.5 and 4.0 respectively. To increase ISR, they are set to 6.0 and 0.25, respectively. These specifications have been widely used in several ATLAS analyses such as the study of $t\bar{t}$ production with a veto on central jet activity [10]. The effects of these changes on the prediction and the comparison to the nominal PYTHIA sample are shown in Fig. 8. The effect of these variations on the b -quark mass is around 20 MeV, which is negligible for the final result, compared to the generator uncertainty.

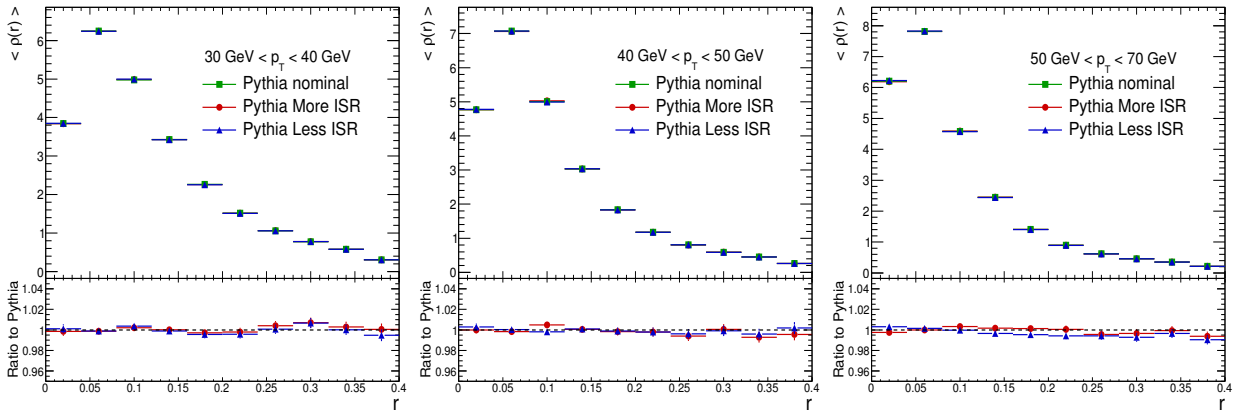


Figure 8: The effects of the initial-state radiation on the b -jet shapes.

7.3. Final-state radiation

The effect of the amount of final-state radiation (FSR) on the b -jet shape distributions is studied by varying the parameters PARP(72) and PARJ(82). These two parameters represent the value of Λ_{QCD} in the time-like showers responsible of the FSR (not arising from a resonant decay), and the infrared invariant mass cutoff, below which partons are not assumed to radiate. To increase the levels of FSR, these values are set to 0.384 and 0.5, respectively. To decrease the FSR activity, they are set to 0.096 and 2.0, respectively. This represents a change of a factor of 2 with respect to their nominal values 0.192 and 1.0. Fig. 9 shows the effect of these variations on the b -jet shapes, as well as the ratio to the nominal PYTHIA prediction. The impact of the FSR on the extracted b -quark mass is around 180 MeV.

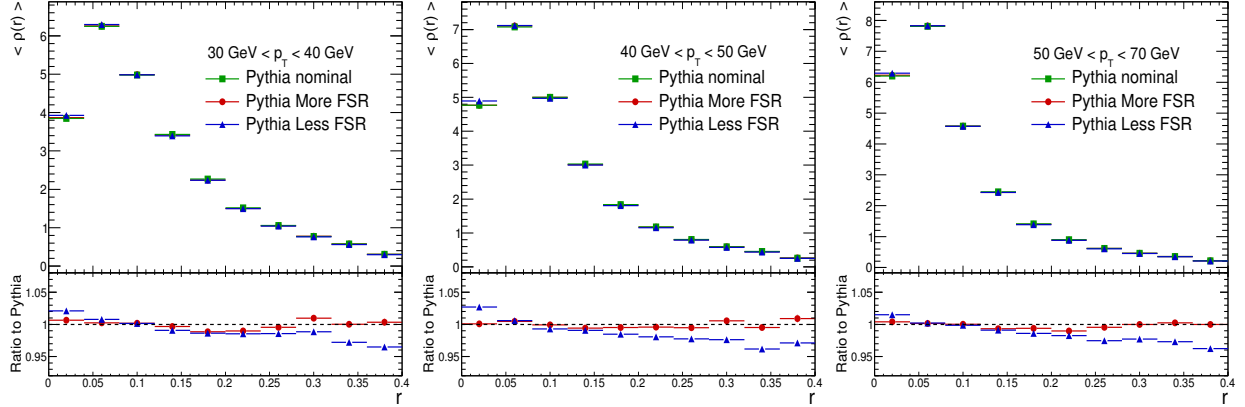


Figure 9: The effects of the final-state radiation on the b -jet shapes.

7.4. Colour reconnection

The effect of the modelling of the colour reconnection (CR) between final-state partons is studied by using the ACR [11] tuning of the PYTHIA Monte Carlo. This tune incorporates a new colour reconnection model, which assumes an enhanced amount of colour connections between partons with respect to the nominal TUNE A sample. Figure 10 shows that the effect of the new CR modelling is to increase the energy deposit on the jet cores on about 2%. The impact on the b -quark mass is estimated by multiplying the nominal predictions by the ratio TUNE ACR/TUNE A, and it has an effect of around 170 MeV.

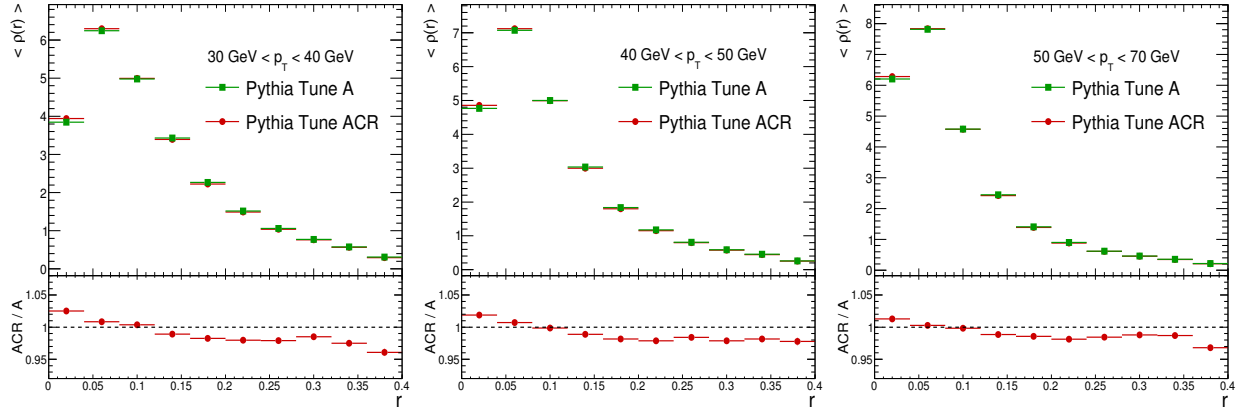


Figure 10: The effects of the colour-reconnection modelling on the b -jet shapes.

7.5. Uncertainty on the Λ_s determination.

The effects of the uncertainties in the determination of the parton shower scale have been also studied. To this end, the full set of m_b variations have been generated again using the values of Λ_s which define the envelope of its determination. Because the value obtained in section 5 was $\Lambda_s = 162.1 \pm 9.6$ MeV, the full scan on m_b variations has been repeated using the values $\Lambda_s = 152.5$ MeV and $\Lambda_s = 171.7$ MeV, which define the endpoints of the interval in which Λ_s can vary due to its experimental uncertainty. This is done in this way, instead of simply shifting each

theoretical prediction by the nominal variation on the jet shapes due to this effect because the jet shapes are highly dependent on both parameters m_b and Λ_s at the same time. To keep track of this correlation, the full set of theoretical predictions has to be recalculated.

The fits with the varied values of Λ_s are then repeated, and the differences between both of them and the central value are taken as the systematic uncertainties on the b -quark mass, which are in principle asymmetric. It is found that the impact on m_b of the determination of the parton shower scale is around 60 MeV at maximum, which represents the 1.2% of the b -quark mass.

Another source of uncertainty related to the way in which Λ_s is determined arises from the fixed order at which the running of α_s is evaluated. To estimate this uncertainty, the value of m_b has been extracted using the running of $\alpha_s(Q^2)$ up to two loops, which is implemented for the HERWIG++ parton shower. The value of the two-loop shower scale was determined to be $\Lambda_s = 276.1 \pm 17.3$ MeV, and the corresponding value of the b -quark mass is $m_b = 5.39 \pm 0.08$ GeV. This value is to be compared with the value obtained for the one-loop running coupling in HERWIG++, which was $m_b = 5.25 \pm 0.09$ GeV, and therefore gives a relative uncertainty of 2.7%. For the nominal value of $m_b = 4.86$ GeV, this represents an additional uncertainty of 0.13 GeV, to be added in quadrature to the result of the propagation of the experimental uncertainty in Λ_s , and therefore has a maximum value of 0.14 GeV.

Discrepancies between data and MC on the description of the transverse momentum of light jets can lead to a biased result on the value of Λ_s . In order to check such effect, the light jet shapes were weighted and the fits were redone. These weights were estimated, in a very conservative way, matching the shape of the p_T distributions of light and b -jets. The differences on Λ_s with respect to the nominal value were found to be small ($\sim 3\%$). This difference is perfectly covered by the error on the fit procedure ($\sim 6\%$), thus ensuring the robustness of the Λ_s determination.

As a further cross-check on the way in which Λ_s is propagated throughout the analysis, the parton shower scale has been determined using the b -jet shapes obtained with the fitted value of m_b . The results are found to be fully compatible with the previous results obtained in Table 2, which reassures us on the extrapolation of Λ_s from light-jets to b -jets.

After the evaluation of the theoretical uncertainties, the final value of the b -quark mass obtained in this analysis can be expressed as

$$m_b = 4.86 \pm 0.08 \text{ (exp.)} \pm 0.39 \text{ (Gen.)} \begin{matrix} +0.02 \\ -0.01 \end{matrix} \text{ (ISR)} \begin{matrix} +0.18 \\ -0.00 \end{matrix} \text{ (FSR)} \begin{matrix} +0.17 \\ -0.00 \end{matrix} \text{ (CR)} \begin{matrix} +0.14 \\ -0.13 \end{matrix} \text{ (PS scale)} . \quad (8)$$

8. Summary and conclusions

This study presents a determination of the mass of the b -quark using jet substructure techniques. It is found that the angular screening effects which were predicted in [4, 5] are confirmed and consistent with a reasonable value of the b -quark mass parameter. The dead cone effect was similarly exploited in [20] to determine the c -quark mass in ep collisions at HERA.

Experimental uncertainties have been propagated using nuisance parameters for each source of uncertainty. This ensures that the correlations between all sources are explicitly taken into account. Systematic effects on the theoretical distributions have also been studied. The modelling of the jet shapes by different Monte Carlo generators is the main uncertainty on this analysis, accounting for an 8% impact on the final value for m_b . Other systematic effects on the theoretical predictions have been studied, such as the amount of initial and final-state radiation, the colour reconnections and the uncertainty on the determination of the parton shower scale Λ_s . Our final result reads

$$m_b = 4.86 \pm 0.08 \text{ (exp.)} \pm 0.39 \text{ (Gen.)} \begin{smallmatrix} +0.02 \\ -0.01 \end{smallmatrix} \text{ (ISR)} \begin{smallmatrix} +0.18 \\ -0.00 \end{smallmatrix} \text{ (FSR)} \begin{smallmatrix} +0.17 \\ -0.00 \end{smallmatrix} \text{ (CR)} \begin{smallmatrix} +0.14 \\ -0.13 \end{smallmatrix} \text{ (PS scale)} . \quad (9)$$

Although there is a significant numerical similarity of this value with the value of the pole mass quoted by the Particle Data Group in [13] and also with the values obtained by the LEP Collaborations in Refs. [21] and [22], the value extracted here should not be confused with the QCD pole mass of the b -quark. It should rather be regarded as the on-shell mass parameter affecting the parton shower kinematics, as calculated in Ref. [7]. In any case, it would be theoretically very interesting to define a way in which the Monte Carlo masses for hadronising quarks can be related to the poles of their respective fermionic propagators.

Acknowledgements. The authors would like to thank Fernando Barreiro and Juan Terrón (UAM) for helpful discussions. We would also like to thank the ATLAS Collaboration for the many invaluable physics measurements already produced and the further to come. Communications with Torbjörn Sjöstrand (Lund) are also thankfully acknowledged.

References

- [1] S.D. Ellis, Z. Kunszt and D. Soper, Phys. Rev. Lett. **69** 3615 (1992). arXiv:hep-ph/9208249.
- [2] I. Vitev, S. Wicks and B-W Zhang, J. High Energy Phys. **811** 093 (2008). arXiv:0810.2807 [hep-ph].
- [3] The ATLAS Collaboration, Eur. Phys. J. C **73** 2676 (2013). arXiv:1307.5749 [hep-ex].
- [4] G. Marchesini and B. R. Webber. Nucl. Phys. **B330** 261-283 (1990).
- [5] Yu L. Dokshitzer, V. A. Khoze and S. I. Troyan. J. Phys. **G17** 1602 (1991).
- [6] T. Sjöstrand, S. Mrenna and P. Skands. JHEP **05** 026 (2006). arXiv:hep-ph/0603175.
- [7] E. Norrbin and T. Sjöstrand, Nucl. Phys. **B603** 297 (2001). arXiv:hep-ph/0010012.
- [8] The ZEUS Collaboration, Nucl. Phys. **B700** 3-50 (2004). arXiv:hep-ex/0405065.
- [9] M. Bahr *et al.* Eur. Phys. J. **C58** 639 (2008). arXiv:0803.0883 [hep-ph].
- [10] The ATLAS Collaboration. Eur. Phys. J. **C72**, 2043 (2012). arXiv:1203.5015 [hep-ex].
- [11] P. Skands and D. Wicke, Eur. Phys. J. **C52**, 133 (2007). arXiv:hep-ph/0703081.
- [12] The Durham HepData project. <http://durpdg.dur.ac.uk/>.
- [13] J. Beringer *et al.* [Particle Data Group], Phys. Rev. **D86** 010001 (2012).
- [14] M. Cacciari, G.P. Salam and G. Soyez JHEP **0804**, 063 (2008). arXiv:0802.1189 [hep-ph].
- [15] M. Cacciari, G.P. Salam and G. Soyez, Eur. Phys. J. **C72** 1896 (2012). arXiv:1111.6097 [hep-ph].
- [16] M. Fischler, D. Sachs. arXiv:hep-ph/0306054.
- [17] J. M. Campbell, E. W. N. Glover and C. J. Maxwell, Phys. Rev. Lett. **81** 1568 (1998). arXiv:hep-ph/9803254.
- [18] The ATLAS Collaboration, Phys. Rev. **D83** 112001 (2011). arXiv:1012.0791 [hep-ex].
- [19] R.D. Field, CDF Note 6403. arXiv:hep-ph/0201192.
- [20] A. Perieanu, DESY-THESIS-2006-002 (2006).
- [21] The DELPHI Collaboration, Eur. Phys. J. **C55** 525-538 (2008). arXiv:0804.3883 [hep-ex].
- [22] The ALEPH Collaboration, Eur. Phys. J. **C18**, 1-13 (2000). arXiv:hep-ex/0008013.